

Superconductive materials with MgB₂-like structures from data-driven screening

Ze Yu^{1,2}, Tao Bo^{1,3}, Bo Liu^{1,2}, Zhendong Fu³, Huan Wang^{4,5}, Sheng Xu^{4,5}, Tianlong Xia^{4,5*},
Shiliang Li^{1,2,3*}, Sheng Meng^{1,2,3*}, Miao Liu^{1,3,6*}

¹Beijing National Laboratory for Condensed Matter Physics, Institute of Physics, Chinese Academy of Sciences, Beijing 100190, China

²School of Physical Sciences, University of Chinese Academy of Sciences, Beijing 100190, China

³Songshan Lake Materials Laboratory, Dongguan, Guangdong 523808, China

⁴Department of Physics, Renmin University of China, Beijing 100872, China

⁵Beijing Key Laboratory of Opto-electronic Functional Materials & Micro-nano Devices, Renmin University of China, Beijing 100872, China

⁶Center of Materials Science and Optoelectronics Engineering, University of Chinese Academy of Sciences, Beijing, 100049, China

*Corresponding author: tlxia@ruc.edu.cn, slli@iphy.ac.cn, smeng@iphy.ac.cn, mliu@iphy.ac.cn

Z. Y. and T. B. contributed equally to this work

Abstract

Finding viable superconducting materials is of interest to the physics community as the superconductors are the playground to manifest many appealing quantum phenomena. This work exemplifies an end-to-end materials discovery towards novel MgB₂-like superconductors, starting from the data-driven compound screening all the way to the experimental materialization. In addition to the known superconducting compounds, CaB₂ ($T_c = 9.4 \sim 28.6$ K), SrGa₂ ($T_c = 0.1 \sim 2.4$ K), BaGa₂ ($T_c = 0.3 \sim 3.3$ K), BaAu₂ ($T_c = 0.0 \sim 0.5$ K), and LaCu₂ ($T_c = 0.1 \sim 2.2$ K) are newly discovered, out of ~182,000 starting structures, to be the most promising superconducting compounds that share similar atomic structures with

MgB₂. Moreover, BaGa₂ is experimentally synthesized and measured to confirm that the compound is a BCS superconductor with $T_c = 0.36$ K, in good agreement with our theoretical predictions. This work provides a “once and for all” study for the MgB₂-like superconductors and showcases that it is feasible to discover new materials via a data-driven approach.

Introduction

Superconductivity is a fascinating and robust quantum phenomenon to manifest the many-body correlations in solids. It was first discovered by Heike and Onnes that mercury became superconductive under 4.2 K[1], then various superconducting materials have been found to have elevated T_c , including niobium-germanium alloy ($T_c = 23.2$ K)[2], lanthanum barium copper oxide ($T_c = 35.0$ K)[3], MgB₂ ($T_c = 39.0$ K)[4], yttrium barium copper oxide ($T_c = 92.0$ K)[5], pressured H₃S ($T_c = 203.5$ K)[6] and, recently, carbonaceous sulfur hydride under pressure ($T_c = 287.7$ K)[7]. Among those systems, MgB₂ possesses superior properties, warranting its great potential for various applications[8]. For example, the high T_c enables the operation of the MgB₂ circuits above 20 K, which is higher than the operating temperature of Nb-based superconducting electronics[9]. In addition, MgB₂ can survive under a high magnetic field than that of Nb-based superconductors, therefore MgB₂ can be utilized as the magnet material in cryogen-free magnetic resonance imaging (MRI) devices[10-14]. Given the appealing advantages of MgB₂, it would be of great interest for the superconductor community to thoroughly screen and evaluate the superconductivity within the MgB₂-like structures.

Taking the advantage of recent progress on materials databases, in this work, we obtain 56 compounds in total that share the same MgB₂-like crystal structure after the intensive structural screening, which is started from ~18k inorganic compounds from the atomly.net. Further screening based on the thermodynamic stability as well as the dynamic stability narrows down the possibility to only 26 compounds. Since MgB₂ was confirmed to satisfy the Bardeen-Cooper-Schrieffer (BCS) theory, the coupling of the electrons to lattice vibrations can be fairly accurately addressed via the first-principles calculations. Hence, all

26 candidates are fed into the following superconducting evaluation at the first-principles level. It is found that the XB_2 ($X = \text{Mg, Al, Ca, Sc, V, Y, Nb, Ta}$), XSi_2 ($X = \text{Ca}$), and XGa_2 ($X = \text{Sr, Ba}$) are superconductive. To validate our approach, one of these compounds, BaGa_2 , has been experimentally made and tested to confirm that the BaGa_2 compound is indeed a superconductor with $T_c = 0.36$ K, in very good agreement with our predictions based on *ab-initio* calculations. This work demonstrates that the BCS superconductors can be discovered in a fairly cost-effective manner through high-throughput computations, and it also provides the superconductor community a viable phase space to search for feasible MgB_2 -like superconductors.

Computation details

The materials data used in this work are obtained from the “atomly.net” [15], an open-access density functional theory (DFT) materials data infrastructure which is conceptually similar to the Materials Project[16], AFLOWlib[17], and OQMD[18]. The data are generated through high-throughput first-principles calculations with an automated workflow to crunch through more than 180,000 inorganic crystal materials. The dataset contains the crystal structure (*e.g.*, crystal structure, X-ray diffraction (XRD)), electronic structure (*e.g.*, the density of states (DOS) and bandgap (E_g)) and energies (*e.g.*, formation energy (E_{form}), energy above the convex hull (E_{hull})) of the compounds, basically all the properties which can be obtained from first-principles calculation. The data are calculated by using the “Vienna Ab Initio Simulation Package” (VASP)[19], and the Perdew-Burke-Ernzerhof (PBE)[20] exchange-correlation functional of generalized gradient approximation (GGA) to deal with the interactions between electrons. The cutoff energy for plane waves is 520 eV, and the k-mesh is $3000/\text{\AA}^3$ or higher.

After the screening, structural optimization is performed for all candidate materials. The plane-wave cutoff was set to be 520 eV with a k-point mesh of $(17 \times 17 \times 15)$ in the Monkhorst-Pack sampling scheme. For geometric optimization, all atoms are allowed to fully relax until the forces on atoms are less than $0.01 \text{ eV}/\text{\AA}$, after considering spin polarization.

The phonon dispersion, electron-phonon coupling (EPC), and superconducting properties are performed using QUANTUM-ESPRESSO (QE) package[21]. The plane-wave kinetic-energy cutoff and the energy cutoff for charge density are set as 100 and 800 Ry, respectively. The Brillouin zone (BZ) k-point mesh of $24 \times 24 \times 24$ and a Methfessel-Paxton smearing width of 0.02 Ry are used to calculate the self-consistent electron density. The dynamic matrix and EPC matrix elements are computed within an $8 \times 8 \times 8$ q mesh. The phonon properties and EPC are calculated based on the density functional perturbation theory (DFPT)[22] and Eliashberg theory[23]. The calculation details are shown in the supplementary materials[24].

Single crystals of BaGa₂ were grown by the self-flux method as reported previously[25]. The resistivity, magnetic susceptibility, and specific heat were measured on a physical property measurement system (PPMS, Quantum Design) with the dilution refrigerator insert.

Results and discussions

In order to comprehensively screen the MgB₂-like materials from the database, the MgB₂ structure (space group P6/mmm, ICSD ID 193379, Materials Project ID mp-763, and atomly ID 0000105522) is used as the structural template. There are two planar layers of atoms in each primitive cell, and the metallic element (X) forms a triangle lattice layer and the non-metallic element (Y) forms the honeycomb lattice layer, and the two planar layers repeat themselves in *c* direction alternatively, forming the stoichiometry of XY₂, as shown in **Fig. 1a**.

A screening process, as shown in **Fig. 1b**, is performed on a dataset of the 182155 materials structures, which is obtained from the atomly.net database, to filter out all the compounds with MgB₂ geometry. An in-house script along with the StructureMatcher module of the Pymatgen library[26] is employed to extract all the compounds with the MgB₂-like structure, and all the radioactive-element-containing compounds are excluded. After the rigorous filtration process, 56 compounds fall out to have the MgB₂-like structure. Then the following screening on the thermodynamic stability narrows down the candidate materials to 51 compounds. The thermodynamic stability of the compounds is assessed by the physical

quantity of energy above hull (E_{hull}), which is the reaction enthalpy required to decompose a material to other stable compounds. The detailed definition of the E_{hull} can be found in ref. [27,28], and thermodynamics-wise, compound with $E_{hull} = 0$ meV/atom is the most stable compound, and the stability is worsening when E_{hull} increases. Out of the 56 candidates, the E_{hull} of 51 structures are smaller than 200 meV/atom, 43 structures are smaller than 100 meV/atom, and 35 structures are smaller than 50 meV/atom. Normally, the threshold of 200 meV/atom is a good value to indicate that the compound is likely to be synthesized, and the 50 meV/atom means the compound is highly likely to be synthesized[29,30]. Finally, the dynamic stability assessment based on phonon spectrum calculations shows that there are 26 dynamically stable materials. They are MgB_2 , AlB_2 , CaB_2 , ScB_2 , TiB_2 , VB_2 , YB_2 , ZrB_2 , NbB_2 , SmB_2 , GdB_2 , TbB_2 , DyB_2 , HoB_2 , ErB_2 , TmB_2 , HfB_2 , TaB_2 , $CaSi_2$, $GdSi_2$, $ErSi_2$, $TmSi_2$, $SrGa_2$, $BaGa_2$, $BaAu_2$, and $LaCu_2$ (see **Fig. S1-4** in the Supplemental Material[24]). Other compounds, BeB_2 , CrB_2 , etc., are found to be dynamically unstable due to the presence of imaginary frequencies in their phonon spectrum. According to the species of anions, these 26 materials can be divided into four categories: the borides XB_2 ($X = Mg, Al, Ca, Sc, Ti, V, Y, Zr, Nb, Sm, Gd, Tb, Dy, Ho, Er, Tm, Hf, Ta$), the silicides XSi_2 ($X = Ca, Gd, Er, Tm$), the gallides XGa_2 ($X = Sr, Ba$) and the alloys ($BaAu_2, LaCu_2$).

According to the existing literature, some of these materials have been extensively studied previously[31-41]. For example, MgB_2 and NbB_2 have been found to transit to superconducting state below 39.0 K and 9.2 K, respectively. Since MgB_2 belongs to the category of conventional superconductors (BCS superconductors), where BCS theory applies, the electron-phonon coupling, as well as the superconducting transition temperature T_c , can be obtained from first-principles calculations.

For the 26 dynamic stable candidates, the EPC constant λ and superconducting transition temperature T_c are obtained from DFPT calculations, as summarized in **Table I**. MgB_2 has the highest calculated T_c of 37.9 K when the empirical parameter μ^* that represents the effective screened-Coulomb-repulsion is 0.04, which is in good agreement with the $T_c = 39$ K obtained in the experiment while tolerating computation errors. Previously, it was found in

experiments that VB_2 [42], TiB_2 [42], and HfB_2 [42] are non-superconductive, in good agreement with our prediction. It was also found that ZrB_2 [31,42], NbB_2 [42-48], and TaB_2 [35,42,49] are superconductive with T_c up to 5.5 K, 9.2 K, and 9.5 K, respectively, confirming our predictions too. In those experiments, the T_c is highly tunable by *non*-stoichiometric ratio, external impurities, etc, hence the experimental values of T_c may still need further investigation. CaSi_2 has a T_c of 14 K when it is under high pressure[50], in line with our predicted value, which is $T_c = 8.7 \sim 16.0$ K. The rare-earth-containing compounds, especially lanthanides (SmB_2 , GdB_2 , TbB_2 , DyB_2 , HoB_2 , ErB_2 , TmB_2 , HfB_2 , GdSi_2 , ErSi_2 , TmSi_2), are not superconductors based on our *ab-initio* calculations, confirming the experimental data[51]. AlB_2 and YB_2 are two exceptions as they are superconductive according to our calculation, but non-superconductive from real-world experiments, therefore they worth in-depth studies.

Other than the compounds mentioned above, the present work adds CaB_2 , SrGa_2 , BaGa_2 , BaAu_2 , and LaCu_2 to the list of compounds within the MgB_2 -structural family, as they have not yet been experimentally examined. Based on our theoretical evaluation, CaB_2 , SrGa_2 , BaGa_2 , BaAu_2 , and LaCu_2 are highly likely to be superconductive, whereas the GdSi_2 , ErSi_2 , and TmSi_2 are non-superconductive. The T_c for CaB_2 , SrGa_2 , BaGa_2 , BaAu_2 , and LaCu_2 , are 9.4 ~ 28.6 K, 0.1 ~ 2.4 K, 0.3 ~ 3.3 K, 0.0 ~ 0.5 K, 0.1 ~ 2.2 K, respectively. Recently, a theoretical work also found that the superconducting transition temperature T_c of BaGa_2 is 1.2 K[52].

To investigate the EPC and superconducting transition temperature T_c of CaB_2 , SrGa_2 , and BaGa_2 , we calculate their phonon dispersion, the phononic density of states (PhDOS), Eliashberg spectral function $\alpha^2F(\omega)$ and cumulative frequency-dependent of EPC constant $\lambda(\omega)$ as presented in **Fig. 2**. For CaB_2 , the Ca vibrations mainly dominate the low frequencies of 0-300 cm^{-1} , while the B vibrations mainly dominate the high frequencies of above 300 cm^{-1} (see **Fig. 2a** and **c**). There are some softened phonon modes along the Γ -A line and around the Γ point at about 350 cm^{-1} , which are associated with the B_{xy} vibration, yielding a large EPC λ_{qv} , as shown in **Fig. 2b**. The phonon dispersion in the frequency range of 300-600 cm^{-1} ,

contributes most to the EPC λ_{qv} (see **Fig. 2d**). The calculated EPC $\lambda(\omega)$ of CaB₂ is 0.75, and when μ^* is 0.14 (the same as for SrGa₂ and BaGa₂), the corresponding T_c is 14.0 K which is quite high in this series of materials.

In SrGa₂ and BaGa₂, some physical properties such as the vibration dominance are quite different. For SrGa₂, the Sr vibrations mainly dominate the low frequencies of 0-120 cm⁻¹, while the Ga vibrations spread in the whole area of the Brillouin zone (BZ) (see **Fig. 2e** and **f**). There is a softened phonon mode around the A point, associated with the Ga_z vibration (~40 cm⁻¹), yielding a large EPC λ_{qv} , as shown in **Fig. 2f**. In addition, the phonon dispersion in the frequency range of 40-120 cm⁻¹, contributes most to the EPC λ_{qv} . The calculated EPC $\lambda(\omega)$ and T_c for SrGa₂ are 0.44 and 0.4 K, respectively. The low-frequency phonons (40-120 cm⁻¹) contribute 86% of the EPC λ , while the high-frequency phonons (180-220 cm⁻¹) contribute about 14% (see **Fig. 2h**). The EPC properties of BaGa₂ are roughly the same as SrGa₂, but relatively stronger. As shown in **Fig. 2i** and **j**, the Ba vibrations mainly dominate the low frequencies of 0-100 cm⁻¹, while the Ga vibrations spread in the whole area of the Brillouin zone (BZ). No imaginary phonon modes indicate that it is dynamically stable, at least from the perspective of the *ab-initio* calculations. As shown in **Fig. 2j** and **l**, the low-frequency phonons (40-100 cm⁻¹) have a large contribution to the EPC λ_{qv} and total EPC λ . The calculated EPC $\lambda(\omega)$ and T_c are 0.56 and 1.3 K, a little lower than those in CaB₂ and SrGa₂.

To validate the high-throughput data-driven prediction based on first principles, the BaGa₂ compound is experimentally synthesized and characterized for its superconductivity. We found that the BaGa₂ is indeed a superconductor with a measured $T_c = 0.36$ K, in good agreement with the theoretical prediction, which is 0.3 ~ 3.3 K. The superconducting properties were measured by resistivity, magnetic-susceptibility, and heat-capacity measurements. **Fig. 3a** shows the temperature dependence of the resistance, which gives the onset T_c of about 0.37 K. Zero resistance is found below 0.29 K. **Fig. 3b** shows the real component of the AC susceptibility χ' as the function of temperature, which exhibits Meissner effect below 0.32 K. **Fig. 3c** further shows the temperature dependence of the specific heat. Above 0.4 K, the specific heat is linearly dependent on the temperature,

demonstrating that the phonon contribution can be neglected below 1 K. A superconducting jump is found at 0.34 K and disappears under 5 kOe. The behavior below T_c can be well fitted by the BCS expression for the specific heat,

$$C = \frac{T}{T_c} \frac{d}{dt} \int_0^\infty dy \left(-\frac{6\gamma\Delta_0}{k_B\pi} \right) [f \ln f + (1-f) \ln (1-f)] \quad (1)$$

where γ is the normal-state Sommerfeld coefficient and f is the Fermi-Dirac distribution function, $f = 1/(e^{E/k_B T} + 1)$. The energy of quasiparticles is given by $E = \sqrt{\epsilon^2 + \Delta^2}$, where ϵ is the energy of the normal electrons relative to Fermi surface. The integration variable is $y = \epsilon/\Delta$. Unlike MgB₂[53], there is no need to introduce two gaps to describe the specific heat data. The fitted value of Δ_0 , the superconducting gap at 0 K, is 0.0433 meV, which gives $2\Delta_0/k_B T_c = 2.83$ with $T_c = 0.355$ K.

The CaB₂, which is predicted to have a higher T_c , has a moderate thermal stability as the E_{hull} is 191 meV/atom, hence, it is harder to be synthesized via the traditional route. Sometimes soft chemistry, template epitaxial growth, or high-pressure synthesis may be able to overcome the unfavorable phase competition. Combining all the information obtained here, SrGa₂, BaAu₂, LaCu₂, and CaB₂, are worth further experimental explorations.

Conclusion

The vast phase space of the MgB₂-like is thoroughly explored to discover new superconductive compounds, leveraging the recent advances of high-throughput computing, materials databases, first-principles calculations as well as state-of-art experiments. This work finds that the SrGa₂, BaGa₂, BaAu₂, and LaCu₂ are promising superconductors, falling out of ~182 thousand starting structures, and of which the BaGa₂ is experimentally synthesized and measured to confirm that the compound is a BCS superconductor with $T_c = 0.36$ K, in line with theoretical predictions. The CaB₂ is predicted to have a higher T_c , but the synthesis can be very challenging. This work provides useful hints for the superconductor

community to search for feasible MgB₂-like BCS superconductors with good performance. From a broad materials science point of view, this work demonstrates an end-to-end materials discovery strategy to forcefully filter out the desired materials via a fast and cost-effective fashion. The “fourth paradigm” data-intensive scientific discovery of promising superconductors is on the radar.

Acknowledgments

The computational resource is provided by the Platform for Data-Driven Computational Materials Discovery of the Songshan Lake laboratory. We especially thank the Atomly database for data sharing. We would also acknowledge the financial support from the Chinese Academy of Sciences (No. ZDBS-LY-SLH007, No. XDB33020000, CAS-WX2021PY-0102), National Science Foundation of China (12025407 and 11934003), and Ministry of Science and Technology (2021YFA1400200).

Supplementary Information

See the Supplementary Information.

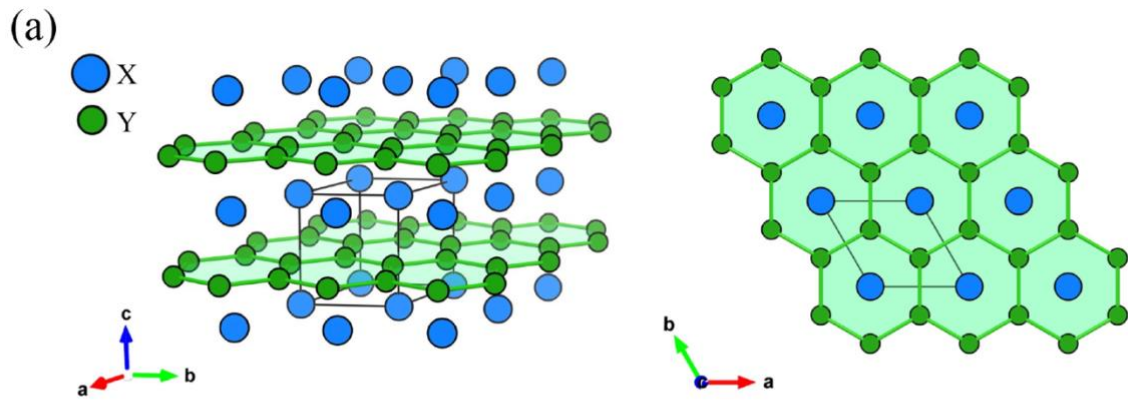
Figure captions

Figure 1. (a) The side & top view of the MgB₂-like materials. (b) The screening flow chart for MgB₂-like materials. The total process is divided into three steps: filtering out all MgB₂-like materials, evaluating thermodynamic stability and dynamics stability. The thermodynamically stable materials are summarized in the table on the right, while the dynamically stable ones are summarized in the table below.

Figure 2. The phonon dispersion weighted by motion modes of constituent elements, the

phonon dispersion weighted by the magnitude of EPC λ_{qv} , PhDOS, Eliashberg spectral function $\alpha^2F(\omega)$ and cumulative frequency-dependent of EPC constant $\lambda(\omega)$ of (a-d) CaB₂, (e-h) SrGa₂, and (i-l) BaGa₂. The red, green, blue, and orange colors in (a & e & i) represent $B_{xy}(G_{xy}, G_{xy})$, $B_z(G_z, G_z)$, $C_{xy}(Sr_{xy}, Ba_{xy})$, and $C_z(Sr_z, Ba_z)$ modes, respectively.

Figure 3 (a) Temperature dependence of the resistivity. Due to the very small resistance, a current of 0.3 mA was used. (b) Temperature dependence of the real component of the AC susceptibility. (c) Temperature dependence of the specific heat at various field. The solid line is fitted by Eq. (1).



(b) 182155 compounds from “Atomly”

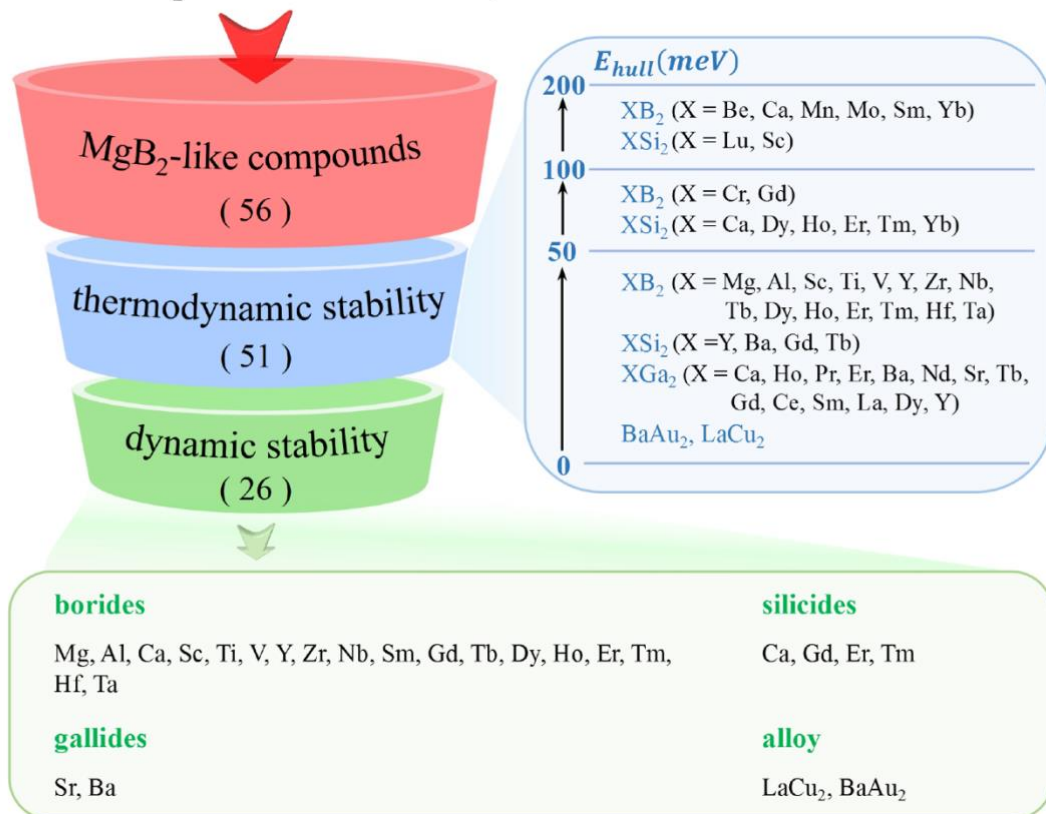


Figure. 1

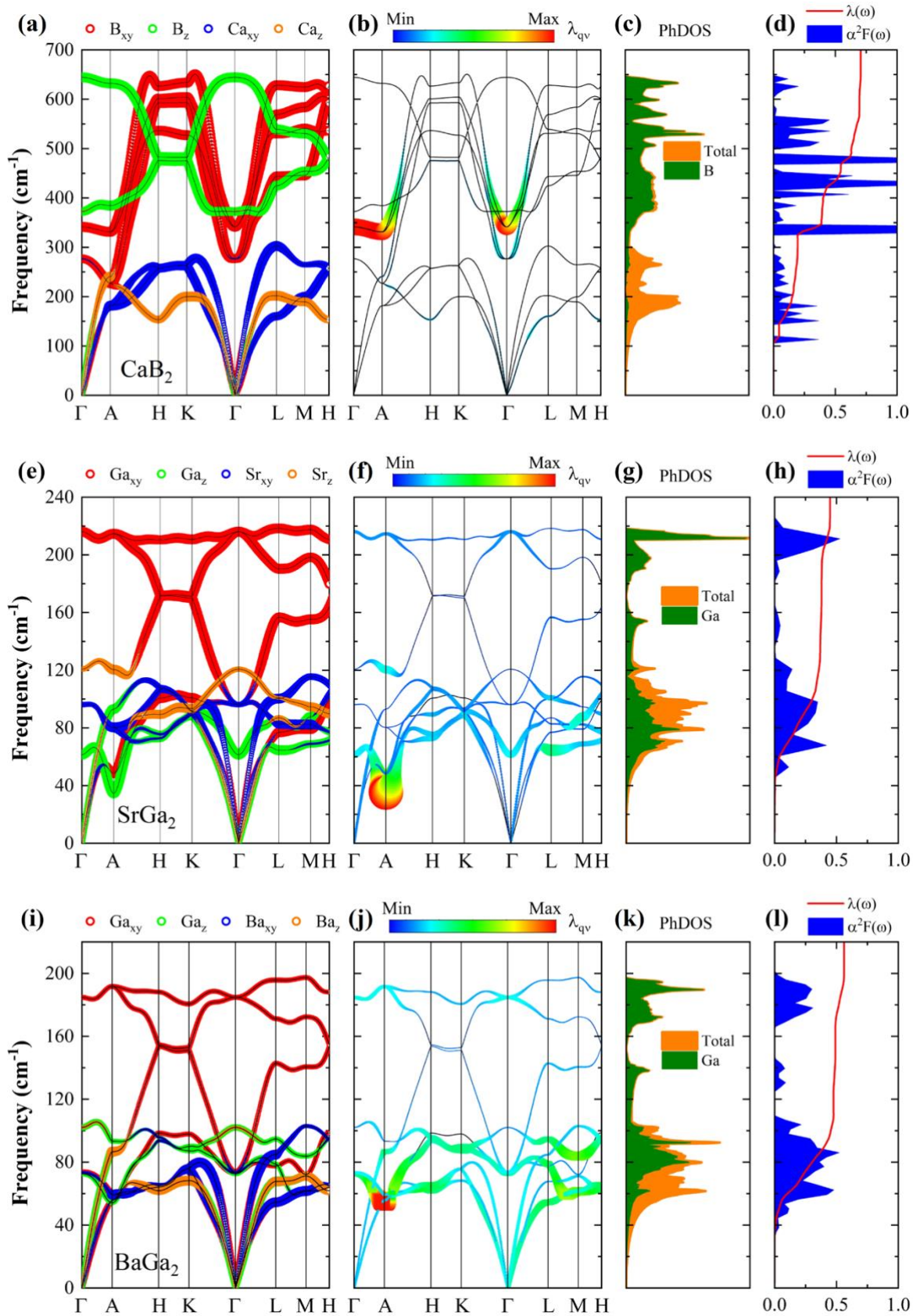


Figure. 2

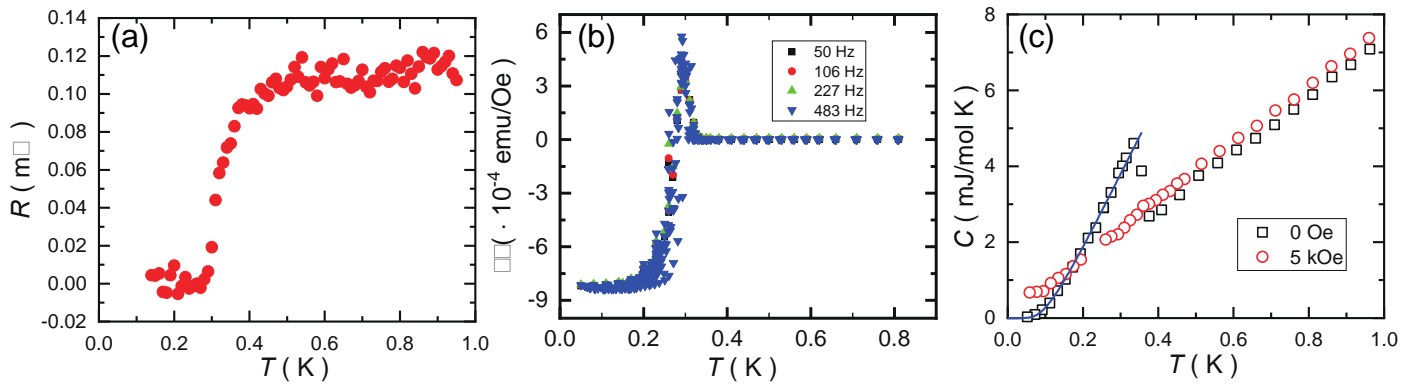


Figure. 3

Table I. The total EPC λ , T_c^{cal} calculated by the *ab-initio* calculations, T_c^{exp} measured by experiments and corresponding references. The empirical parameter μ^* representing effective shielding of Coulomb rejection ranges from 0.04 to 0.18. Symbol notes: “/” means or, “~” means within this range, “-” means no corresponding data.

Formula	λ	T_c^{cal} (K)	T_c^{exp} (K)	Reference
MgB₂	0.68	10.3 ~ 37.9	39.0	[4]
AlB₂	0.47	0.6 ~ 10.9	0.0	[54]
CaB₂	0.75	9.4 ~ 28.6	-	-
ScB₂	0.28	0.0 ~ 1.7	1.5	[55,56]
TiB₂	0.13	0.0 ~ 0.0	0.0	[42]
VB₂	0.36	0.0 ~ 4.2	0.0	[42]
YB₂	0.40	0.1 ~ 6.1	0.0	[57]
ZrB₂	0.14	0.0 ~ 0.0	0.0 / 5.5	[31,42]
NbB₂	0.71	5.7 ~ 19.4	0.6 ~ 9.2	[42-48]
SmB₂	0.08	0.0 ~ 0.0	0.0	[51]
GdB₂	0.15	0.0 ~ 0.0	0.0	[51]
TbB₂	0.12	0.0 ~ 0.0	0.0	[51]
DyB₂	0.11	0.0 ~ 0.0	0.0	[51]
HoB₂	0.10	0.0 ~ 0.0	0.0	[51]
ErB₂	0.09	0.0 ~ 0.0	0.0	[51]
TmB₂	0.10	0.0 ~ 0.0	0.0	[51]
HfB₂	0.14	0.0 ~ 0.0	0.0	[42]
TaB₂	0.95	9.4 ~ 20.3	0.0 / 9.5	[35,42,49]
CaSi₂	1.13	8.7 ~ 16.0	14.0	[50]
GdSi₂	0.07	0.0 ~ 0.0	-	-
ErSi₂	0.09	0.0 ~ 0.0	-	-
TmSi₂	0.12	0.0 ~ 0.0	-	-
SrGa₂	0.44	0.1 ~ 2.4	-	-
BaGa₂	0.56	0.3 ~ 3.3	-	-
BaAu₂	0.34	0.0 ~ 0.5	-	-
LaCu₂	0.46	0.1 ~ 2.2	-	-

References

- [1] H. K. Onnes, in *KNAW, Proceedings* 1911), pp. 1910.
- [2] J. R. Gavaler, Superconductivity in Nb–Ge films above 22 K, *Appl. Phys. Lett.* **23**, 480 (1973).
- [3] J. G. Bednorz and K. A. Müller, Possible high T_c superconductivity in the Ba-La-Cu-O system, *Zeitschrift für Physik B Condensed Matter* **64**, 189 (1986).
- [4] J. Nagamatsu, N. Nakagawa, T. Muranaka, Y. Zenitani, and J. Akimitsu, Superconductivity at 39 K in magnesium diboride, *Nature* **410**, 63 (2001).
- [5] M. K. Wu, J. R. Ashburn, C. J. Torng, P. H. Hor, R. L. Meng, L. Gao, Z. J. Huang, Y. Q. Wang, and C. W. Chu, Superconductivity at 93 K in a new mixed-phase Y-Ba-Cu-O compound system at ambient pressure, *Phys. Rev. Lett.* **58**, 908 (1987).
- [6] A. P. Drozdov, M. I. Eremets, I. A. Troyan, V. Ksenofontov, and S. I. Shylin, Conventional superconductivity at 203 kelvin at high pressures in the sulfur hydride system, *Nature* **525**, 73 (2015).
- [7] E. Snider, N. Dasenbrock-Gammon, R. McBride, M. Debessai, H. Vindana, K. Vencatasamy, K. V. Lawler, A. Salamat, and R. P. Dias, Room-temperature superconductivity in a carbonaceous sulfur hydride, *Nature* **586**, 373 (2020).
- [8] M. Tomsic, M. Rindfleisch, J. Yue, K. Mcfadden, J. Phillips, M. D. Sumption, M. Bhatia, S. Bohnenstiehl, and E. W. Collings, Overview of MgB₂ Superconductor Applications, *International Journal of Applied Ceramic Technology* **4**, 250 (2007).
- [9] D. Cunnane, K. Chen, and X. X. Xi, Superconducting MgB₂ rapid single flux quantum toggle flip flop circuit, *Appl. Phys. Lett.* **102**, 222601 (2013).
- [10] M. Modica, S. Angius, L. Bertora, D. Damiani, M. Marabotto, D. Nardelli, M. Perrella, M. Razeti, and M. Tassisto, Design, construction and tests of MgB₂ coils for the development of a cryogen free magnet, *IEEE transactions on applied superconductivity* **17**, 2196 (2007).
- [11] C. Poole, T. Baig, R. J. Deissler, D. Doll, M. Tomsic, and M. Martens, Numerical study on the quench propagation in a 1.5 T MgB₂ MRI magnet design with varied wire compositions, *Supercon. Sci. Technol.* **29**, 044003 (2016).
- [12] J. Ling, J. P. Voccio, S. Hahn, T. Qu, J. Bascuñán, and Y. Iwasa, A persistent-mode 0.5 T solid-nitrogen-cooled MgB₂ magnet for MRI, *Supercon. Sci. Technol.* **30**, 024011 (2016).
- [13] T. Baig, A. Al Amin, R. J. Deissler, L. Sabri, C. Poole, R. W. Brown, M. Tomsic, D. Doll, M. Rindfleisch, and X. Peng, Conceptual designs of conduction cooled MgB₂ magnets for 1.5 and 3.0 T full body MRI systems, *Supercon. Sci. Technol.* **30**, 043002 (2017).
- [14] D. Patel, A. Matsumoto, H. Kumakura, M. Maeda, S.-H. Kim, H. Liang, Y. Yamauchi, S. Choi, J. H. Kim, and M. S. A. Hossain, Superconducting joints using multifilament MgB₂ wires for MRI application, *Scripta Materialia* **204**, 114156 (2021).
- [15] Atomly, <https://atomly.net>.
- [16] A. Jain, S. P. Ong, G. Hautier, W. Chen, W. D. Richards, S. Dacek, S. Cholia, D. Gunter, D. Skinner, G. Ceder, and K. A. Persson, Commentary: The Materials Project: A materials genome approach to accelerating materials innovation, *APL Materials* **1**, 011002 (2013).
- [17] S. Curtarolo, W. Setyawan, G. L. W. Hart, M. Jahnatek, R. V. Chepulskii, R. H. Taylor, S. Wang, J. Xue, K. Yang, O. Levy, M. J. Mehl, H. T. Stokes, D. O. Demchenko, and D. Morgan, AFLOW: An automatic framework for high-throughput materials discovery, *Computational Materials Science* **58**, 218 (2012).
- [18] J. E. Saal, S. Kirklin, M. Aykol, B. Meredig, and C. Wolverton, Materials Design and Discovery with High-Throughput Density Functional Theory: The Open Quantum Materials Database (OQMD), *JOM* **65**, 1501 (2013).
- [19] G. Kresse and J. Furthmüller, Efficient iterative schemes for ab initio total-energy calculations using a plane-wave basis set, *Phys. Rev. B* **54**, 11169 (1996).
- [20] J. P. Perdew, K. Burke, and M. Ernzerhof, Generalized Gradient Approximation Made Simple, *Phys. Rev. Lett.* **77**, 3865 (1996).
- [21] P. Giannozzi, S. Baroni, N. Bonini, M. Calandra, R. Car, C. Cavazzoni, D. Ceresoli, G. L. Chiarotti, M. Cococcioni, and I. Dabo, QUANTUM ESPRESSO: a modular and open-source software project for quantum simulations of materials, *Journal of physics: Condensed matter* **21**, 395502 (2009).
- [22] S. Baroni, S. De Gironcoli, A. Dal Corso, and P. Giannozzi, Phonons and related crystal properties from density-functional perturbation theory, *Rev. Mod. Phys.* **73**, 515 (2001).

- [23]F. Giustino, Electron-phonon interactions from first principles, *Rev. Mod. Phys.* **89** (2017).
- [24]See Supplemental Material at [URL will be inserted by publisher] for Phonon spectrums.
- [25]S. Xu, C. Bao, P.-J. Guo, Y.-Y. Wang, Q.-H. Yu, L.-L. Sun, Y. Su, K. Liu, Z.-Y. Lu, S. Zhou, and T.-L. Xia, Interlayer quantum transport in Dirac semimetal BaGa₂, *Nat Commun* **11** (2020).
- [26]S. P. Ong, W. D. Richards, A. Jain, G. Hautier, M. Kocher, S. Cholia, D. Gunter, V. L. Chevrier, K. A. Persson, and G. Ceder, Python Materials Genomics (pymatgen): A robust, open-source python library for materials analysis, *Computational Materials Science* **68**, 314 (2013).
- [27]S. P. Ong, L. Wang, B. Kang, and G. Ceder, Li-Fe-P-O₂ Phase Diagram from First Principles Calculations, *Chemistry of Materials* **20**, 1798 (2008).
- [28]A. Jain, G. Hautier, S. P. Ong, C. J. Moore, C. C. Fischer, K. A. Persson, and G. Ceder, Formation enthalpies by mixing GGA and GGA+U calculations, *Phys. Rev. B* **84** (2011).
- [29]M. Liu, A. Jain, Z. Rong, X. Qu, P. Canepa, R. Malik, G. Ceder, and K. A. Persson, Evaluation of sulfur spinel compounds for multivalent battery cathode applications, *Energy & Environmental Science* **9**, 3201 (2016).
- [30]M. Aykol, S. S. Dwaraknath, W. Sun, and K. A. Persson, Thermodynamic limit for synthesis of metastable inorganic materials, *Science advances* **4**, eaaq0148 (2018).
- [31]V. A. Gasparov, N. S. Sidorov, I. I. Zver'Kova, and M. P. Kulakov, Electron transport in diborides: Observation of superconductivity in ZrB₂, *Journal of Experimental and Theoretical Physics Letters* **73**, 532 (2001).
- [32]D. Kaczorowski, J. Klamut, and A. Zaleski, Some comments on superconductivity in diborides, *arXiv preprint cond-mat/0104479* (2001).
- [33]N. I. Medvedeva, A. L. Ivanovskii, J. E. Medvedeva, and A. J. Freeman, Electronic structure of superconducting MgB₂ and related binary and ternary borides, *Phys. Rev. B* **64** (2001).
- [34]P. Ravindran, P. Vajeeston, R. Vidya, A. Kjekshus, and H. Fjellvåg, Detailed electronic structure studies on superconducting MgB₂ and related compounds, *Phys. Rev. B* **64** (2001).
- [35]H. Rosner, W. E. Pickett, S.-L. Drechsler, A. Handstein, G. Behr, G. Fuchs, K. Nenkov, K.-H. Müller, and H. Eschrig, Electronic structure and weak electron-phonon coupling in TaB₂, *Phys. Rev. B* **64** (2001).
- [36]G. Satta, G. Profeta, F. Bernardini, A. Continenza, and S. Massidda, Electronic and structural properties of superconducting MgB₂, CaSi₂, and related compounds, *Phys. Rev. B* **64** (2001).
- [37]S. Elgazzar, P. M. Oppeneer, S.-L. Drechsler, R. Hayn, and H. Rosner, Calculated de Haas-van Alphen data and plasma frequencies of MgB₂ and TaB₂, *Solid State Commun.* **121**, 99 (2002).
- [38]T. Takahashi, S. Kawamata, S. Noguchi, and T. Ishida, Superconductivity and crystal growth of NbB₂, *Physica C: Superconductivity* **426-431**, 478 (2005).
- [39]H. J. Choi, S. G. Louie, and M. L. Cohen, Prediction of superconducting properties of CaB₂ using anisotropic Eliashberg theory, *Phys. Rev. B* **80** (2009).
- [40]S. Okatov, A. Ivanovskii, Y. E. Medvedeva, and N. Medvedeva, The electronic band structures of superconducting MgB₂ and related borides CaB₂, MgB₆ and CaB₆, *physica status solidi (b)* **225**, R3 (2001).
- [41]T. Oguchi, Cohesion in AlB₂-type diborides: a first-principles study, *J. Phys. Soc. Jpn.* **71**, 1495 (2002).
- [42]L. Leyarovska and E. Leyarovski, A search for superconductivity below 1 K in transition metal borides, *Journal of the Less Common Metals* **67**, 249 (1979).
- [43]A. Yamamoto, C. Takao, T. Masui, M. Izumi, and S. Tajima, High-pressure synthesis of superconducting Nb_{1-x}B₂ (x=0-0.48) with the maximum T_c=9.2 K, *Physica C: Superconductivity* **383**, 197 (2002).
- [44]H. Takeya, K. Togano, Y. S. Sung, T. Mochiku, and K. Hirata, Metastable superconductivity in niobium diborides, *Physica C: Superconductivity* **408**, 144 (2004).
- [45]J. K. Hulm and B. T. Matthias, New Superconducting Borides and Nitrides, *Phys. Rev.* **82**, 273 (1951).
- [46]W. T. Ziegler and R. A. Young, Studies of Compounds for Superconductivity, *Phys. Rev.* **90**, 115 (1953).

- [47] J. E. Schirber, D. L. Overmyer, B. Morosin, E. L. Venturini, R. Baughman, D. Emin, H. Klesnar, and T. Aselage, Pressure dependence of the superconducting transition temperature in single-crystal NbB_x ($x \text{ near } 2$) with $T_c = 9.4$ K, *Phys. Rev. B* **45**, 10787 (1992).
- [48] H. Kotegawa, K. Ishida, Y. Kitaoka, T. Muranaka, N. Nakagawa, H. Takagiwa, and J. Akimitsu, Evidence for strong-coupling s-wave superconductivity in MgB_2 : ^{11}B -NMR study of MgB_2 and the related materials, *Physica C: Superconductivity* **378-381**, 25 (2002).
- [49] D. Kaczorowski, A. Zaleski, O. Żogał, and J. Klamut, Incipient superconductivity in TaB_2 , arXiv preprint cond-mat/0103571 (2001).
- [50] S. Sanfilippo, H. Elsinger, M. Núñez-Regueiro, O. Laborde, S. Lefloch, M. Affronte, G. L. Olcese, and A. Palenzona, Superconducting high pressure CaSi_2 phase with $T_{c\text{up}}$ to 14 K, *Phys. Rev. B* **61**, R3800 (2000).
- [51] S. Gabani, K. Flachbart, K. Siemensmeyer, and T. Mori, Magnetism and superconductivity of rare earth borides, *Journal of Alloys and Compounds* **821**, 153201 (2020).
- [52] C. Parlak, The physical properties of AlB_2 -type structures CaGa_2 and BaGa_2 : An ab-initio study, *Physica B: Condensed Matter* **576**, 411724 (2020).
- [53] F. Bouquet, R. A. Fisher, N. E. Phillips, D. G. Hinks, and J. D. Jorgensen, Specific Heat of MgB_2 : Evidence for a Second Energy Gap, *Phys. Rev. Lett.* **87** (2001).
- [54] K.-P. Bohnen, R. Heid, and B. Renker, Phonon dispersion and electron-phonon coupling in MgB_2 and AlB_2 , *Phys. Rev. Lett.* **86**, 5771 (2001).
- [55] G. V. Samsonov and I. M. Vinitskii, *Handbook of refractory compounds* (Springer, 1980).
- [56] S. M. Sichkar and V. N. Antonov, Electronic structure, phonon spectra and electron-phonon interaction in ScB_2 , *Low Temperature Physics* **39**, 595 (2013).
- [57] A. S. Cooper, E. Corenzwit, L. D. Longinotti, B. T. Matthias, and W. H. Zachariasen, Superconductivity: The Transition Temperature Peak Below Four Electrons per Atom, *Proceedings of the National Academy of Sciences* **67**, 313 (1970).